




High-power pre-chirp managed amplification of circularly polarized pulses using high-dispersion chirped mirrors as a compressor

YAO ZHANG,^{1,2,8} RUNZHI CHEN,^{2,8} HANGDONG HUANG,^{1,2} YIZHOU LIU,³ HAO TENG,² SHAOBO FANG,² WEI LIU,⁴ FRANZ KAERTNER,³  JUNLI WANG,^{1,5}  GUOQING CHANG,^{2,6} AND ZHIYI WEI^{1,2,7} 

¹*School of Physics and Optoelectronic Engineering, Xidian University, Xi'an 710071, China*

²*Beijing National Laboratory for Condensed Matter Physics, Institute of Physics, Chinese Academy of Sciences, Beijing 100190, China*

³*Center for Free-Electron Laser Science, DESY, Notkestraße 85, 22607 Hamburg, Germany*

⁴*School of Physics and Astronomy, Sun Yat-Sen University, Zhuhai 519082, China*

⁵*dispersion@126.com*

⁶*guoqing.chang@iphy.ac.cn*

⁷*zywei@iphy.ac.cn*

⁸*These authors contributed equally to this work*

Abstract: We incorporate two techniques into pre-chirp managed amplification (PCMA) to achieve high-energy ultrashort pulses with the duration well below 100 fs. Numerical simulations confirmed by our experimental results demonstrate that seeding PCMA with circularly polarized pulses instead of linearly polarized pulses can increase the amplified pulse energy by 1.5 times. We also employ high-dispersion chirped mirrors to compress the amplified pulses with the throughput efficiency as high as 98%. These two techniques allow us to demonstrate an Yb-fiber PCMA system that emits 50-MHz, 47-fs pulses with 101.2-W average power.

© 2020 Optical Society of America under the terms of the [OSA Open Access Publishing Agreement](#)

1. Introduction

An Yb-fiber laser system that incorporates chirped-pulse amplification (CPA) has become a mature platform to generate high power and high energy ultrafast pulses [1,2]. Sufficient stretching (up to several ns) ensures that the seeding pulses are almost linearly amplified to the energy level up to ~1 mJ [3,4]. The amplified pulses are compressed by a pair of diffraction gratings that are spatially separated by about 1-m distance. Due to the gain narrowing effect, the amplified pulses normally exhibit a narrower optical spectrum compared with the seeding pulses; as a result, the compressed pulses are of ~200 fs in duration [4,5]. In addition to linear amplification by CPA, Yb-fiber amplifiers that amplify seeding pulses in a nonlinear manner are under intensive investigation. Nonlinear amplification utilizes the fiber-optic nonlinearity to overcome the gain-bandwidth limit such that the seeding pulses are spectrally broadened during the amplification. Consequently, the amplified pulses can be compressed by a grating pair to a duration well below 100 fs. These nonlinear amplification techniques include parabolic pulse amplification [6–10], pre-chirp managed amplification (PCMA) [11–19], and gain-managed nonlinear amplification [20], to name a few. Among nonlinear amplification methods, PCMA allows flexibly pre-chirping the seeding pulses and therefore can deliver compressed pulses as short as 24 fs [17]. PCMA implemented in rod-type Yb-fiber amplifiers featuring large-mode-area can produce microjoule level, tens-of-fs pulses with 100-W level average power [14–16,18].

Current implementation of high power PCMA suffers from two drawbacks: (1) higher nonlinearity due to amplification of linearly polarized seeding pulses and (2) considerable power loss associated with grating-pair based compressor. In this paper, we overcome these two drawbacks by seeding a PCMA Yb-fiber amplifier with circularly polarized pulses and compressing the amplified pulses by high-dispersion chirped mirrors (HDCMs). As is well known, the nonlinear refraction coefficient corresponding to circularly polarized pulses is $2/3$ of that for linearly polarized pulses [21,22]. Intuitively we expect that switching to circular polarization for the seeding pulses may readily scale up the amplified pulse energy by a factor of 1.5. For an ultrafast laser aiming for high average-power (i.e., >100 W), the loss due to pulse compression should be kept minimal. In current implementation, nearly all the Yb-fiber amplification systems—whether linear or nonlinear—adopt grating-pair based compressors that exhibit normally $>20\%$ throughput loss [3,4,14,18,19,23]. Noticeable spatial chirp and pulse front tilt may arise from grating misalignment leading to compromised beam quality. In contrast, chirped mirrors are made of multi-layer dielectric coatings and feature negligible reflection loss [24,25]. Though widely used in solid-state lasers for dispersion control, the group-delay dispersion (GDD) of chirped mirrors is about 1000 times less than a diffraction-grating pair. Therefore, a fiber CPA system—in which the amplified pulses are as long as 1 ns—cannot employ chirped mirrors for pulse compression. In contrast, the amplified pulses from a PCMA fiber amplifier are as short as about 1 ps and therefore pulse compression using chirped mirrors is entirely possible.

In this paper, we investigate the effect of seeding-pulse polarization in an Yb-fiber PCMA system. Using both numerical simulation and detailed experiments, we show that, under the same condition, circularly polarized pulses accumulate the least nonlinear phase during the nonlinear amplification compared with linear or elliptical polarization. As a result, seeding a PCMA with circularly polarized pulses rather than linearly polarized pulses can increase the energy of the amplified pulses by a factor of 1.5. Meanwhile, we compress the amplified pulses using home designed HDCMs with an efficiency of 98%. To the best of our knowledge, this represents the first demonstration that chirped-mirror based compressor can be used in a fiber amplifier system. Incorporating these two techniques (circularly polarized seeding and HDCMs based compressor), our Yb-fiber PCMA system delivers 50-MHz, 47-fs pulses with 101.2-W average power.

2. Configuration of Yb-fiber PCMA system with circularly polarized seeding pulses and HDCM-based compressor

Figure 1 shows the experimental schematic setup of our PCMA system, which consists of four parts: fiber laser frontend, pre-chirping device, power amplifier, and HDCM based compressor. The fiber laser frontend provides 50-MHz positively chirped pulses centered at 1036 nm with 7-W average power. A half-wave plate (HWP) combined with a polarization beam splitter (PBS) varies the power coupled into the amplifier. A pair of transmission-gratings (groove density: 1000 lines/mm) prior to the power amplification adjusts the pre-chirp of the pulses. These linearly polarized pulses center at 1036 nm with a full-width-at-half-maximum (FWHM) of 6.4 nm. After properly pre-chirped, the pulses are then amplified in a 0.8-m Yb-doped rod-type photonic crystal fiber (PCF) with a core diameter of 85 μm . We place a quarter-wave plate (QWP) before the PCF to convert linearly polarized pulses into their circularly polarized counterparts. At the PCF output, another QWP converts the circular polarization back to the linear polarization before compression. The amplified pulses are finally compressed by several home-designed HDCMs.

Figure 2 illustrates the coating structure of the HDCM that includes 55 alternating layers of Nb_2O_5 and SiO_2 . The measured group-delay as a function of wavelength is plotted as inset, showing that each bounce provides a dispersion of about -2000 fs^2 at $1.03 \mu\text{m}$.

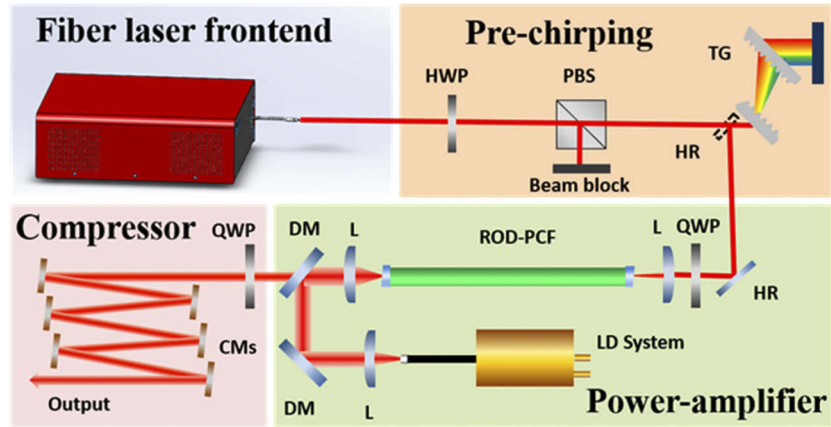


Fig. 1. Schematic of the experimental setup. HWP: half-wave plate, QWP: quarter-wave plate, PBS: polarization beam splitter, HR: high reflection mirror, PCF: photonic crystal fiber, L: plane convex lens, LD: laser diode, TG: transmission grating, DM: dichroic mirror, CMs: chirped mirrors.

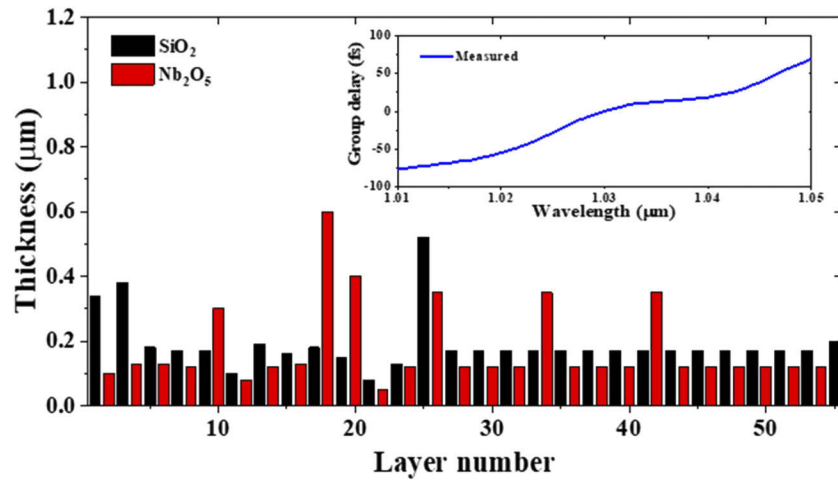


Fig. 2. Structure and performance of home-designed chirped mirror featuring high dispersion.

3. Modeling of PCMA seeded by pulses with arbitrary polarization

Amplification of circularly polarized pulses has been experimentally implemented in Yb-fiber CPA systems, in which the fiber-optic nonlinearity is detrimental and should be minimized. In contrast, PCMA exploits nonlinearity for broadening the amplified spectrum. To better understand how pulses with different polarization states evolve in an Yb-fiber PCMA system, we model such a nonlinear amplifier using the following coupled generalized nonlinear Schrödinger equations [26]:

$$\frac{\partial U_1}{\partial z} - \sum_{k \geq 2} \frac{i^{k+1} \beta_k}{k!} \frac{\partial^k U_1}{\partial \tau^k} = \frac{1}{L_{NL}} \left(i - \frac{1}{\omega_0} \frac{\partial}{\partial \tau} \right) \left(f_R U_1 \int_{-\infty}^{\infty} h_R(\tau - \tau') [|U_1(\tau')|^2 + |U_2(\tau')|^2] d\tau' + (1 - f_R) U_1 \left[\frac{2}{3} |U_1|^2 + \frac{4}{3} |U_2|^2 \right] \right) + \frac{g}{2} U_1 \quad (1)$$

$$\frac{\partial U_2}{\partial z} - \sum_{k \geq 2} \frac{i^{k+1} \beta_k}{k!} \frac{\partial^k U_2}{\partial \tau^k} = \frac{1}{L_{NL}} \left(i - \frac{1}{\omega_0} \frac{\partial}{\partial \tau} \right) \left(f_R U_2 \int_{-\infty}^{\infty} h_R(\tau - \tau') [|U_2(\tau')|^2 + |U_1(\tau')|^2] d\tau' + (1 - f_R) U_2 \left[\frac{2}{3} |U_2|^2 + \frac{4}{3} |U_1|^2 \right] \right) + \frac{g}{2} U_2 \quad (2)$$

$U_1(z, \tau)$ and $U_2(z, \tau)$ denote the right-handed circular polarization (RHCP) eigenstate and left-handed circular polarization (LHCP) eigenstate, respectively. They are normalized by the square root of incident peak power (i.e., $\sqrt{P_0}$). β_k represents the k^{th} -order fiber dispersion. L_{NL} is the nonlinear length defined as $L_{NL} = 1/(\gamma P_0)$, γ where is the nonlinear parameter $\gamma = \omega_0 n_2 / c A_{\text{eff}}$. ω_0 is the center frequency, n_2 the nonlinear-index coefficient of $2.6 \times 10^{-20} \text{ m}^2/\text{W}$ in fused silica, c the light speed in vacuum, and A_{eff} the mode-field area. $f_R = 0.18$ represents the fractional contribution of the Raman response and $h_R(t)$ denotes the Raman response function. g in the last term on the right-hand side represents the gain coefficient of the fiber amplifier.

An input pulse $U(z=0, \tau)$ normalized by $\sqrt{P_0}$ can be decomposed into a superposition of two eigenvectors—the RHCP eigenvector \hat{e}_1 and the LHCP eigenvector \hat{e}_2 —with different weights $U_1(z=0, \tau)$ and $U_2(z=0, \tau)$: $U = \hat{e}_1 U_1 + \hat{e}_2 U_2$. For an input pulse that may be of arbitrary polarization, we introduce parameter *ellipticity* defined as

$$e = \frac{|U_1| - |U_2|}{|U_1| + |U_2|}. \quad (3)$$

Equation (3) gives the ratio of the short axis to long axis of the optical ellipse. Table 1 lists different polarizations and their corresponding e values.

Table 1. Different polarization states of U and corresponding e values

Polarization	Left-handed circular	Left-handed elliptical	Linear	Right-handed elliptical	Right-handed circular
Ellipticity	$e = -1$	$-1 < e < 0$	$e = 0$	$0 < e < 1$	$e = 1$

In the simulation, without loss of generality, we assume that the input pulse has an optical spectrum of Gaussian profile centered at 1036 nm with a FWHM of 5.3 nm. Such a spectrum supports 300-fs transform-limited Gaussian pulse. At the input, we add -50000 fs^2 GDD to the optical spectrum such that the transform-limited pulse is pre-chirped to 551 fs in duration. Table 2 lists the simulation parameters for investigating the polarization effect in an Yb-fiber PCMA system.

Figure 3(a) shows the spectral evolution of linearly polarized pulses amplified from 44 nJ to 1.4 μJ . Because the seeding pulses are negatively pre-chirped the spectrum becomes narrower at the initial amplification [27,28]; after propagating in the fiber amplifier for about 32 cm, the spectrum reaches the narrowest FWHM of about 3.3 nm. Further propagation in the amplifier is accompanied by dramatic spectral broadening. At the output of the fiber amplifier, the spectrum has a bandwidth of 43.3 nm. Such a broad spectrum supports transform-limited pulses of 44 fs in duration. To show the effect of pulse polarization, we redo the simulation in which circularly polarized pulses are amplified from 44 nJ to 1.4 μJ ; the results are shown in Fig. 3(b). A comparison between Figs. 3(a) and 3(b) shows that amplification of circularly or linearly polarized

Table 2. Parameters in the simulation for modeling Yb-fiber PCMA system.

Input pulse	
Center wavelength	1036 nm
Spectral profile	Gaussian
Spectral bandwidth (FWHM)	5.3 nm @ 1036 nm
GDD added to the optical spectrum for pre-chirping the input pulse	-50000 fs ²
Pulse duration (negatively pre-chirped)	551 fs
Power amplifier (from NKT, aeroGAIN-ROD)	
Fiber length	80 cm
Fiber mode-field diameter (MFD)	65 μ m
Total power gain	15 dB
Group-velocity dispersion, β_2	20 fs ² /mm
Third-order dispersion, β_3	40 fs ³ /mm
Nonlinear refractive index, n_2	2.6×10^{-20} m ² /W

pulses follows similar evolution. However, due to less nonlinearity during the amplification, the spectrum of circularly polarized pulses at the amplifier output has a smaller bandwidth of 35.7 nm. To show that amplification of circularly polarized pulses can increase the amplified pulse energy by a factor of 1.5, we carry out another simulation in which circularly polarized pulses are amplified from 66 nJ to 2.1 μ J [Fig. 3(c)]. As we expect, the spectral evolution in Fig. 3(c) is nearly identical to the one in Fig. 3(a), which indicates that, given the same spectral bandwidth at the amplifier output, circularly polarized pulses exhibit 1.5 times more energy compared with linearly polarized pulses.

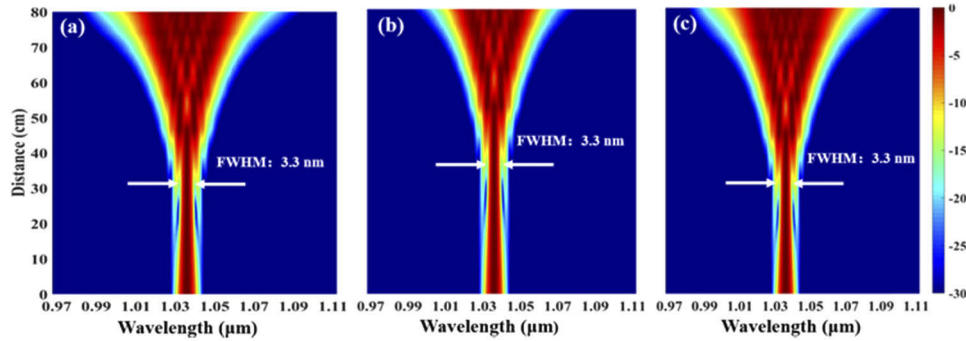


Fig. 3. Effect of seeding polarization on spectral evolution inside the pre-chirp managed Yb-fiber amplifier. (a) Amplification of linearly polarized pulses from 44 nJ to 1.4 μ J. (b) Amplification of circularly polarized pulses from 44 nJ to 1.4 μ J. (c) Amplification of circularly polarized pulses from 66 nJ to 2.1 μ J. The spectral intensity is normalized and shown in logarithmic scale. White arrows in each figure indicates the narrowest bandwidth.

In Fig. 3, we only compare amplification of seeding pulses that are linearly or circularly polarized pulses. What happens if the seeding pulses are elliptically polarized? To answer this question, we perform a simulation in which an elliptically polarized pulse is amplified from 44 nJ to 1.4 μ J. The seeding pulse is elliptically polarized with $e = 0.52$ (i.e., $|U_1|^2 = 10|U_2|^2$), implying that the seeding pulse corresponds to superposition of a RHCP pulse with 40-nJ energy and a LHCP pulse with 4-nJ energy.

Figures 4(a) and 4(b) illustrate the spectral evolution of the RHCP eigenstate and the LHCP eigenstate, respectively. While evolving in a similar manner as those in Fig. 3, these two eigenstates develop different spectral bandwidth. The red (blue) curve in Fig. 4(c) plots the spectrum of the RHCP (LHCP) eigenstate at the amplifier output; black curve represents the total spectrum of the amplified elliptical pulse. Surprisingly the LHCP eigenstate has a larger bandwidth than the RHCP eigenstate although the latter has 10 times more pulse energy. This is because the spectral broadening arises from a combination of self-phase modulation (SPM) and cross-phase modulation (XPM). Since the RHCP eigenstate is one order of magnitude stronger than the LHCP one, the RHCP eigenstate is spectrally broadened mainly by SPM and the LHCP one by XPM. As Eqs. (1) and (2) show, the strength of XPM is twice as much as that of SPM, and therefore the weaker LHCP eigenstate develops a broader spectrum at the amplifier output than the RHCP eigenstate does. As is well known, Kerr nonlinearity causes nonlinear polarization evolution if the input seeding pulse to a fiber amplifier is elliptically polarized. This is evidenced by the black curve in Fig. 4(d), which shows that the ellipticity becomes wavelength dependent. For a comparison, the dotted curve in the same figure indicates the ellipticity (0.52) corresponding to the pulse at amplifier input. Such a wavelength dependent ellipticity implies that different spectrum components correspond to different polarization states. As a result, the amplified pulse cannot be converted into a linearly polarized pulse by a QWP without introducing energy loss.

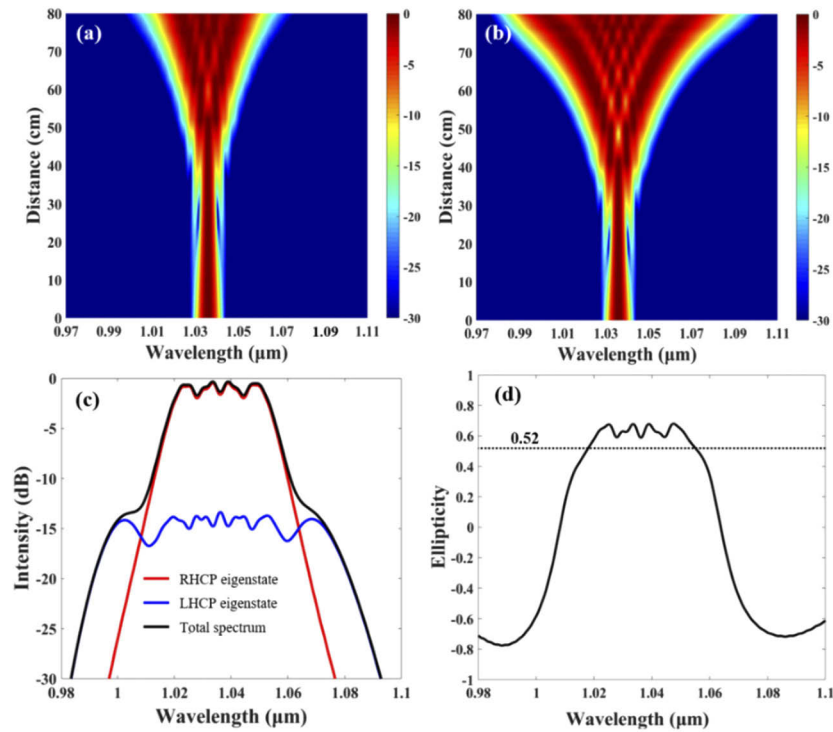


Fig. 4. Amplification of elliptically polarized seeding pulses from 44 nJ to 1.4 μJ in Yb-fiber PCMA system. The seeding pulse corresponds to superposition of a RHCP pulse with 40-nJ energy and a LHCP pulse with 4-nJ energy. (a) Spectral evolution of RHCP eigenstate. (b) Spectral evolution of LHCP eigenstate. (c) Red curve: spectrum of RHCP eigenstate, Blue curve: spectrum LHCP eigenstate, and black curve: total spectrum. (d) Ellipticity as a function of wavelength for the amplified pulse. Dotted curve: ellipticity at the amplifier input.

In contrast, nonlinear polarization evolution is absent when the seeding pulses are linearly or circularly polarized. Especially circularly polarized pulses maintain the polarization state during the amplification, and a QWP at the amplifier output can conveniently convert the amplified pulses to be linearly polarized without causing loss. Therefore, in the following experiments, we seed our Yb-fiber PCMA with pulses either linearly polarized or circularly polarized, and compare their performance in terms of energy scalability and pulse compression.

4. Experimental results

Guided by above simulations, we carry out detailed experimental investigation. We first amplify circularly polarized pulses from 3.2 W to 55 W. Before the amplification, we carefully adjust the grating pair to add -60000-fs^2 GDD to the optical spectrum. As the simulation results show, the nonlinear phase shift accumulated inside the fiber amplifier determines the spectral evolution. Because we cannot perform a cut-back experiment to obtain how the spectrum evolves along the amplifier fiber (as shown in Fig. 3), we adjust the pump power to vary the amplifier output power, which in turn changes the accumulated nonlinear phase shift to the amplified pulse. As Fig. 5(a) shows, the amplified spectrum becomes narrower at low power and the bandwidth decreases from initial 7.6 nm to 2.1 nm when amplified to 10-W average power. Further increasing the power leads to a broader spectrum: at 55-W average power, the bandwidth is 19.3 nm.

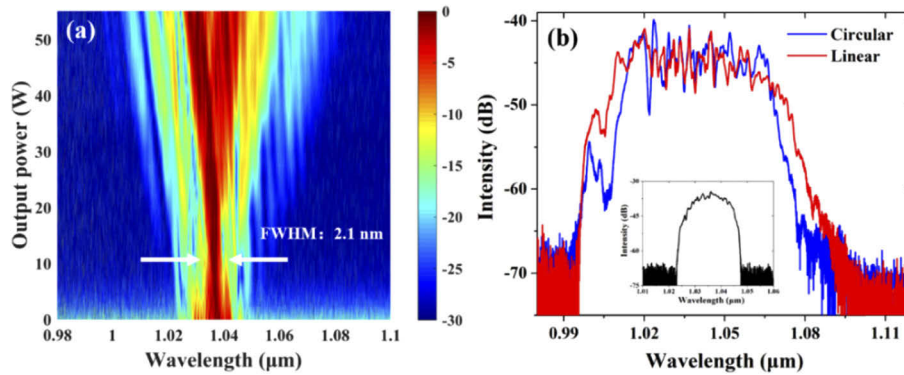


Fig. 5. (a) Spectral evolution of circularly polarized pulses when amplified up to 55 W. (b) Amplified spectra at 60-W average power. Blue curve: circularly polarized pulse, red curve: linearly polarized pulse. Inset: spectrum of input pulse before the amplifier.

To make a direct comparison of amplification of linearly and circularly polarized pulses, we rotate the QWP before the power amplifier to adjust input polarization while maintaining the coupled power unchanged. By properly adjusting the pre-chirp to -36000 fs^2 , we obtain two different spectra at 60-W output power shown in Fig. 5(b); the inset is the optical spectrum of the input pulse. The blue (red) curve corresponds to the amplified spectrum of the circularly (linearly) polarized pulses. Apparently, linearly polarized pulses develop a broader amplified spectrum than the circularly polarized pulses do.

To show 1.5 times energy improvement associated with PCMA seeded by circularly polarized pulses, we seed our Yb-fiber PCMA with pulses either linearly polarized or circularly polarized and compare their performance in terms of energy scalability and pulse compression. The red curve in Fig. 6(a) shows the output spectra at 50-W average power when the PCMA is seeded by 2.1-W linearly polarized pulses that are pre-chirped by adding -20000-fs^2 GDD. Then we adjust the seed pulses to be circularly polarized and increase the input power to 3.15 W (1.5 times 2.1 W), and the optical spectrum for the amplified pulses at 75-W average power is plotted as the blue curve. The good overlap between the blue and red curves indicate that seeding PCMA using

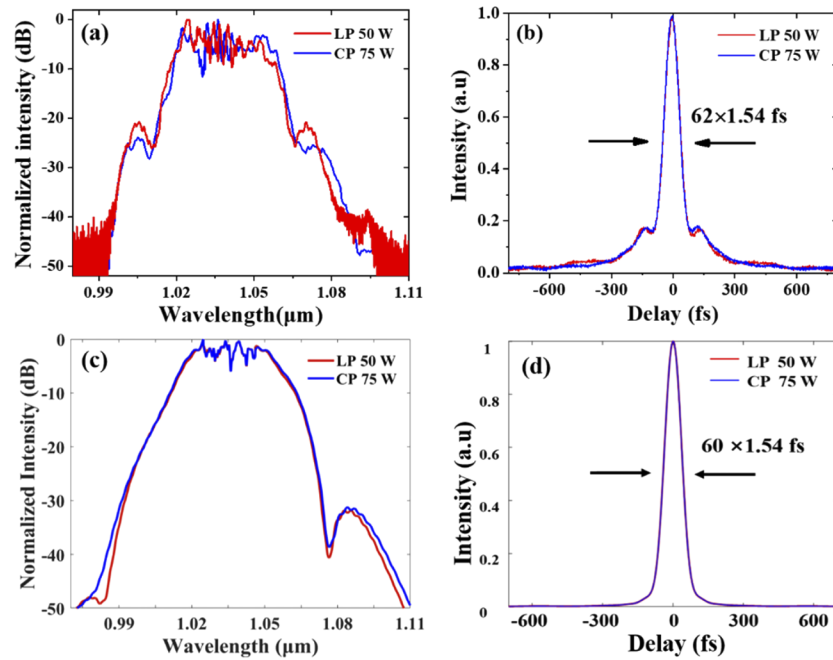


Fig. 6. (a) Measured spectra of 50-W linearly polarized pulses (red curve) and 75-W circularly polarized pulses (blue curve). (b) Measured autocorrelation traces of the compressed pulses. Red curve: 50-W linearly polarized pulses, Blue curve: 75-W circularly polarized pulses. (c) Simulated spectra of 50-W linearly polarized pulses (red curve) and 75-W circularly polarized pulses (blue curve). (d) Simulated autocorrelation traces for the compressed pulses. Red curve: 50-W linearly polarized pulses, Blue curve: 75-W circularly polarized pulses.

circularly polarized pulses does increase pulse energy by 1.5 times for the amplified spectra with

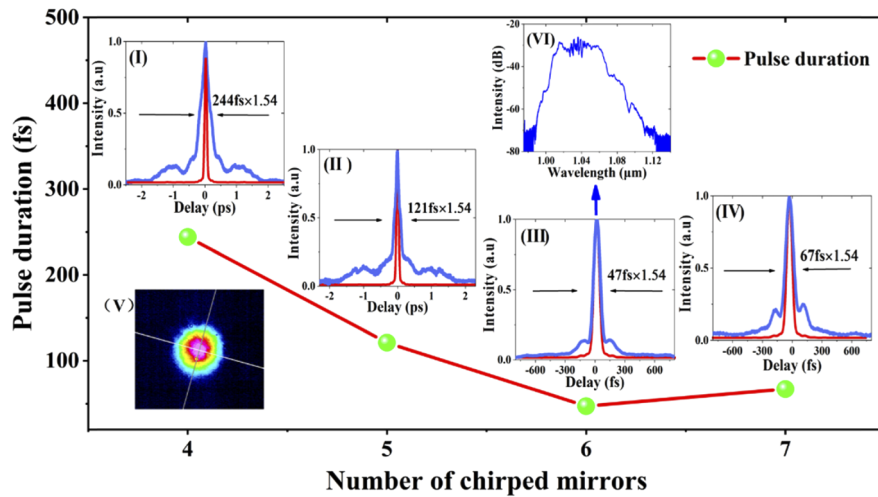


Fig. 7. Measured autocorrelation traces of the compressed pulses versus the number of HDCMs. In the experiment, 3.2-W circularly polarized pulses are amplified to 103.4-W average power.

the same bandwidth. To show that these two spectra indeed develop nearly the same phase as well, we compress the amplified pulses by compensating for the spectral phase using 6 HDCMs. The compressed pulses are measured by an intensity autocorrelator; the measured autocorrelation traces corresponding to 50-W linearly polarized pulses and 75-W circularly polarized pulses are plotted in Fig. 6(b) as red curve and blue curve, respectively. These nearly overlapped curves confirm that the two spectra have almost identical phase and the duration of the compressed pulses is estimated to be about 62 fs assuming hyperbolic secant pulse profile.

To further verify these experimental results, we simulate our experiment by feeding Eqs. (1) and (2) with measured data (e.g., input spectrum, pre-chirping GDD, pulse energy). Figure 6(c) shows the calculated spectra corresponding to 50-W linearly polarized pulses (red curve) and 75-W circularly polarized pulses (blue curve). A comparison between the results in Fig. 6(a) and 6(c) shows a quantitative agreement between experiments and simulation. To simulate pulse compression, we numerically introduce a compressor that adds to the spectrum a quadratic phase corresponding to -12000-fs^2 GDD. Figure 6(d) plots the calculated autocorrelation traces of the compressed pulses in linear polarization (red curve, 50-W average power) and circular polarization (blue curve, 75-W average power). The two autocorrelation traces almost completely overlap with each other, and they quantitatively agree with the experimental results presented in Fig. 6(b).

Supported by above results, we further increase the pump power to amplify the circularly polarized pulses from 3.15 W to 103.4 W. Subsequently, the amplified pulses are converted back to linear polarization with the polarization extinction ratio exceeding 15 dB. Figure 7 plots the measured autocorrelation traces (blue curves in inset I to IV) versus the number of chirped mirrors. Calculated autocorrelation traces for the corresponding transform-limited pulses (red curves) are used to evaluate the compression quality. The best compression is achieved using 6 HDCMs with >98% efficiency, which delivers 101.2-W, 47-fs compressed pulses; in this case, the pre-chirping GDD is -32000 fs^2 . The excellent beam profile and optical spectrum are shown in inset V and inset VI, respectively.

5. Conclusion

In summary, we theoretically and experimentally investigate evolution of seeding pulses at different polarization in a PCMA system. Both simulation and experimental results indicate that employing circularly polarized pulses rather than linearly polarized pulses allows convenient energy improvement by a factor of 1.5 without sacrificing the compressed-pulse quality. We further demonstrate that HDCMs with negligible loss can be used to compress amplified pulses in a PCMA system thanks to their intrinsic short pulse duration. Equipped by these two techniques, our Yb-fiber PCMA system produces 101.2-W, 47-fs pulses at 50-MHz repetition rate. Energy scaling of fiber PCMA system is ultimately limited by self-focusing that causes catastrophic damage to the gain fiber. At $1.03\text{ }\mu\text{m}$, the self-focusing critical power is $\sim 4\text{ MW}$ for linearly polarized pulses and $\sim 6\text{ MW}$ for circularly polarized pulses. Given that the duration of the amplified pulses is about 1 ps, the maximum pulse energy that can be achieved from an Yb-fiber PCMA seeded by circularly polarized pulses is about $6\text{ }\mu\text{J}$. Further energy scaling can be achieved by incorporating coherent combining techniques (e.g., divided pulse amplification and spatial beam combination); the resulting fiber PCMA system may deliver $\sim 30\text{-fs}$ pulses with $>30\text{-}\mu\text{J}$ (i.e., 1-GW peak power) pulse energy and kW average power. Such a laser source constitutes an enabling tool for high-field applications such as driving high-harmonic generation to obtain high-flux photons at the extreme ultra-violet wavelength.

Funding

Key-Area Research and Development Program of Guangdong Province (2018B090904003); National Key Research and Development Program of China (2017YFC0110301); National

Natural Science Foundation of China (11774234, 91950113, 61575219, 11674386, 61675158); Youth Innovation Promotion Association of the Chinese Academy of Sciences (2018007); Open Research Fund of State Key Laboratory of Pulsed Laser Technology.

Disclosures

The authors declare no conflicts of interest.

References

1. A. Galvanauskas, "Mode-scalable fiber-based chirped pulse amplification systems," *IEEE J. Sel. Top. Quantum Electron.* **7**(4), 504–517 (2001).
2. J. Limpert, F. Roser, D. N. Schimpf, E. Seise, T. Eidam, S. Hadrich, J. Rothhardt, C. J. Misas, and A. Tünnemann, "High Repetition Rate Gigawatt Peak Power Fiber Laser-Systems: Challenges, Design, and Experiment," *IEEE J. Sel. Top. Quantum Electron.* **15**(1), 159–169 (2009).
3. F. Roser, T. Eidam, J. Rothhardt, O. Schmidt, D. N. Schimpf, J. Limpert, and A. Tünnemann, "Millijoule pulse energy high repetition rate femtosecond fiber chirped-pulse amplification system," *Opt. Lett.* **32**(24), 3495–3497 (2007).
4. T. Eidam, J. Rothhardt, F. Stutzki, F. Jansen, S. Haedrich, H. Carstens, C. Jauregui, J. Limpert, and A. Tünnemann, "Fiber chirped-pulse amplification system emitting 3.8 GW peak power," *Opt. Express* **19**(1), 255–260 (2011).
5. W. Zhao, X. Hu, and Y. Wang, "Femtosecond-pulse fiber based amplification techniques and their applications," *IEEE J. Sel. Top. Quantum Electron.* **20**(5), 512–524 (2014).
6. M. E. Fermann, V. I. Kruglov, B. C. Thomsen, J. M. Dudley, and J. D. Harvey, "Self-Similar Propagation and Amplification of Parabolic Pulses in Optical Fibers," *Phys. Rev. Lett.* **84**(26), 6010–6013 (2000).
7. J. Limpert, T. Schreiber, T. Clausnitzer, K. Zöllner, H. J. Fuchs, E. B. Kley, H. Zellmer, and A. Tünnemann, "High-power femtosecond Yb-doped fiber amplifier," *Opt. Express* **10**(14), 628–638 (2002).
8. D. N. Papadopoulos, Y. Zaouter, M. Hanna, F. Druon, E. Mottay, E. Cormier, and P. Georges, "Generation of 63 fs 4.1 MW peak power pulses from a parabolic fiber amplifier operated beyond the gain bandwidth limit," *Opt. Lett.* **32**(17), 2520–2522 (2007).
9. Y. Zaouter, D. N. Papadopoulos, M. Hanna, J. Boulet, L. Huang, C. Aguergaray, F. Druon, E. Mottay, P. Georges, and E. Cormier, "Stretcher-free high energy nonlinear amplification of femtosecond pulses in rod-type fibers," *Opt. Lett.* **33**(2), 107–109 (2008).
10. B. Nie, D. Pestov, F. W. Wise, and M. Dantus, "Generation of 42-fs and 10-nJ pulses from a fiber laser with self-similar evolution in the gain segment," *Opt. Express* **19**(13), 12074–12080 (2011).
11. H.-W. Chen, J. Lim, S.-W. Huang, D. N. Schimpf, F. X. Kärtner, and G. Chang, "Optimization of femtosecond Yb-doped fiber amplifiers for high-quality pulse compression," *Opt. Express* **20**(27), 28672–28682 (2012).
12. J. Lim, H.-W. Chen, G. Chang, and F. X. Kärtner, "Frequency comb based on a narrowband Yb-fiber oscillator: pre-chirp management for self-referenced carrier envelope offset frequency stabilization," *Opt. Express* **21**(4), 4531–4538 (2013).
13. J. Zhao, W. Li, C. Wang, Y. Liu, and H. Zeng, "Pre-chirping management of a self-similar Yb-fiber amplifier towards 80 W average power with sub-40 fs pulse generation," *Opt. Express* **22**(26), 32214–32219 (2014).
14. W. Liu, D. N. Schimpf, T. Eidam, J. Limpert, A. Tünnemann, F. X. Kärtner, and G. Chang, "Pre-chirp managed nonlinear amplification in fibers delivering 100 W, 60 fs pulses," *Opt. Lett.* **40**(2), 151–154 (2015).
15. Y. Liu, W. Li, D. Luo, D. Bai, C. Wang, and H. Zeng, "Generation of 33 fs 93.5 W average power pulses from a third-order dispersion managed self-similar fiber amplifier," *Opt. Express* **24**(10), 10939–10945 (2016).
16. D. Luo, W. Li, Y. Liu, C. Wang, Z. Zhu, W. Zhang, and H. Zeng, "High-power self-similar amplification seeded by a 1 GHz harmonically mode-locked Yb-fiber laser," *Rev. Sci. Instrum.* **87**(9), 093114 (2016).
17. H. Song, B. Liu, Y. Li, Y. Song, H. He, L. Chai, M. Hu, and C. Wang, "Practical 24-fs, 1-μJ, 1-MHz Yb-fiber laser amplification system," *Opt. Express* **25**(7), 7559–7566 (2017).
18. D. Luo, Y. Liu, C. Gu, C. Wang, Z. Zhu, W. Zhang, Z. Deng, L. Zhou, W. Li, and H. Zeng, "High-power Yb-fiber comb based on pre-chirped-management self-similar amplification," *Appl. Phys. Lett.* **112**(6), 061106 (2018).
19. Y. Hua, G. Chang, F. X. Kärtner, and D. N. Schimpf, "Pre-chirp managed, core-pumped nonlinear PM fiber amplifier delivering sub-100-fs and high energy (10 nJ) pulses with low noise," *Opt. Express* **26**(5), 6427–6438 (2018).
20. P. Sidorenko, W. Fu, and F. Wise, "Nonlinear ultrafast fiber amplifiers beyond the gain-narrowing limit," *Optica* **6**(10), 1328 (2019).
21. D. N. Schimpf, T. Eidam, E. Seise, S. Haedrich, J. Limpert, and A. Tünnemann, "Circular versus linear polarization in laser-amplifiers with Kerr-nonlinearity," *Opt. Express* **17**(21), 18774–18781 (2009).
22. X. Chen, A. Jullien, A. Malvache, L. Canova, A. Borot, A. Trisorio, C. G. Durfee, and R. Lopez-Martens, "Generation of 4.3 fs, 1 mJ laser pulses via compression of circularly polarized pulses in a gas-filled hollow-core fiber," *Opt. Lett.* **34**(10), 1588–1590 (2009).
23. T. Eidam, S. Hanf, E. Seise, T. V. Andersen, T. Gabler, C. Wirth, T. Schreiber, J. Limpert, and A. Tünnemann, "Femtosecond fiber CPA system emitting 830 W average output power," *Opt. Lett.* **35**(2), 94–96 (2010).

24. J. R. Birge and F. X. Kärtner, "Phase distortion ratio: alternative to group delay dispersion for analysis and optimization of dispersion compensating optics," *Opt. Lett.* **35**(14), 2469–2471 (2010).
25. H.-W. Chen, T. Sosnowski, C.-H. Liu, L.-J. Chen, J. R. Birge, A. Galvanauskas, F. X. Kärtner, and G. Chang, "Chirally-coupled-core Yb-fiber laser delivering 80-fs pulses with diffraction-limited beam quality warranted by a high-dispersion mirror based compressor," *Opt. Express* **18**(24), 24699–24705 (2010).
26. H. Tu, Y. Liu, J. Laegsgaard, D. Turchinovich, M. Siegel, D. Kopf, H. Li, T. Gunaratne, and S. A. Boppert, "Nonlinear polarization dynamics in a weakly birefringent all-normal dispersion photonic crystal fiber: toward a practical coherent fiber supercontinuum laser," *Opt. Express* **20**(2), 1113–1128 (2012).
27. M. Oberthaler and R. A. Höpfel, "Spectral narrowing of ultrashort laser pulses by self-phase modulation in optical fibers," *Appl. Phys. Lett.* **63**(8), 1017–1019 (1993).
28. B. R. Washburn, J. A. Buck, and S. E. Ralph, "Transform-limited spectral compression due to self-phase modulation in fibers," *Opt. Lett.* **25**(7), 445–447 (2000).